Prutkin Ilya, Peter Vajda, Jo Gottsmann, 2014. The gravimetric picture of magmatic and hydrothermal sources driving hybrid unrest on Tenerife in 2004/5. *Journal of Volcanology and Geothermal Research*, 282: 9–18,
doi 10.1016/j.jvolgeores.2014.06.003 **preprint**
Final published ms (e-offprint): http://www.sciencedirect.com/science/article/pii/S0377027314001784

The gravimetric picture of magmatic and hydrothermal sources driving hybrid unrest on Tenerife in 2004/5

PRUTKIN Ilya[1], VAJDA Peter[2,*], GOTTSMANN Jo[3]

* corresponding author

Abstract
We present results from the inversion of gravity changes observed at the central volcanic complex (CVC) of Tenerife, Canary Islands, between May 2004 and July 2005. Marking a period of elevated activity and a reawakening of the volcanic system, the data depict spatial and temporal variations in the sub-surface processes that defined this period of unrest at the Pico Viejo (PV) – Pico Teide (PT) complex, after the last volcanic eruption on Tenerife in 1909. An initial non-linear inversion, based on 3D line segments approximation, yielded three line segments at depths between 1 km a.s.l. and 2 km b.s.l. Our interpretation of the initial inversion results is that the line segments represent apparent composite sources, a superposition of deep and shallow seated sources. We therefore decomposed the gravity changes into shallow and deep parts (fields) using a procedure based on triple harmonic continuation. The shallow and deep fields could then be inverted separately, using the same inversion methodology. The deep field constrains two connected line segments at the depth of about 6 km b.s.l., in the center of the NW seismogenic zone of VT events swarm of the seismic unrest, that we interpret as magma input. The inversion of the shallow field images three weak line segments that are all situated at very shallow, near-surface depths. We interpret the weak segments as hydrothermal sources potentially excited by the deeper magma injection. Our results indicate no significant input into the shallow phonolitic plumbing system of the PV–PT complex, but rather a deeper-seated rejuvenation of the mafic feeder reservoir. The emerging picture from our analysis is that the 2004/5 unrest on Tenerife was of a hybrid nature due to the combination of a deep magma injection (failed eruption?) coupled with fluid migration to shallow depths. The identified causative link between deep and shallow unrest sources indicates the presence of permeable pathways for shallow fluid migration at the CVC.

Keywords: gravity change interpretation, Pico Viejo–Pico Teide, volcano reactivation, nonlinear inversion, line segments approximation

1. Introduction and Background

The central volcanic complex (CVC) on Tenerife (Fig. 1), Canary Islands, is a young (< 175 ka) volcanic complex situated within the Las Cañadas caldera (LCC), dominated by the twin-volcanoes of Pico Viejo (PV) and Pico Teide (PT). The complex has erupted rock suites from basanitic to phonolitic compositions (Ablay and Marti, 2000). In contrast, the Santiago rift zone (SRZ), which extends towards the NW from the PV-PT complex, is dominated by mostly monogenetic mafic volcanism. The most recent magmatic eruption on Tenerife was the formation of the Chinyero scoria cone in 1909 in the center of the SRZ. A notable deviation from the background on-shore seismic activity started in April 2004 including a number of felt earthquakes (García et al., 2006; Tárraga et al., 2006; Almendros et al., 2007; Cerdeña et al., 2011). Other indicators for

[1] Institute of Geosciences, Jena University, Burgweg 11, D-07749 Jena, Germany
[2] Geophysical Institute, Slovak Academy of Sciences, Dubravska cesta 9, 845 28 Bratislava, Slovakia, Peter.Vajda@savba.sk, Tel.: +421 2 59410 603, Fax: +421 2 59410 607
[3] Department of Earth Sciences, University of Bristol, Bristol, UK

Prutkin Ilya, Peter Vajda, Jo Gottsmann, 2014. The gravimetric picture of magmatic and hydrothermal sources driving hybrid unrest on Tenerife in 2004/5. *Journal of Volcanology and Geothermal Research*, 282: 9–18,
doi 10.1016/j.jvolgeores.2014.06.003 **preprint**
Final published ms (e-offprint): http://www.sciencedirect.com/science/article/pii/S0377027314001784

volcanic unrest were anomalous gas emissions (Pérez et al., 2005; García et al., 2006; Melián et al., 2012), and spatio-temporal gravity changes (Gottsmann et al., 2006). Despite marked changes in these monitoring parameters, no statistically significant surface deformation (either inflation or deflation) was observed. Unrest continued through 2005 along with a significant decrease in the number of recorded earthquakes from a peak of more than 400 events in May 2004 to around 100 events per month by mid-2005 (e.g., Cerdeña et al., 2011).

Simultaneous to the increased seismic activity, a bulk gravity increase was recorded across a network of observation points at the CVC by Gottsmann et al. (2006), who attributed the mass changes between May 2004 and July 2005 to the migration of fluids as a result of a tentative dyke intrusion into the CVC in April 2004. Almendros et al. (2007) proposed a model for the unrest based on seismic data whereby a deep magma injection triggered a release of fluids into an overlying aquifer. Exploiting a new seismic catalogue, Cerdeña et al. (2011), propose a multiple source model for the 2004/5 unrest, and suggest a complex succession of deep and shallow seated magmatic intrusions beneath the CVC between 2001 and 2005. The initial interpretation of the spatio-temporal gravity changes by Gottsmann et al. (2006) was based on a single source inversion of gravity changes, neglecting the possibility of multiple causative sources for the observed unrest. Multiple sources contributing to unrest were identified for example at the Campi Flegrei, caldera from spatio-temporal gravity and deformation data (Gottsmann et al., 2006), where shallow-seated and quickly evolving sources appear to dominate gravity variations along the structural borders of the caldera, most probably related to fluid flow. Here, we test the hypothesis of source-multiplicity for the recorded gravity time series on Tenerife to shed further light on the cause and nature of the unrest in 2004/5 using a nonlinear inversion method based on 3D line segments approximation. A thorough exploitation of the limited available data documenting this non-eruptive unrest is vital for the understanding of source processes and the characterization of future unrest events on Tenerife, where geophysical timeseries spanning pre-eruptive and eruptive activity are absent.

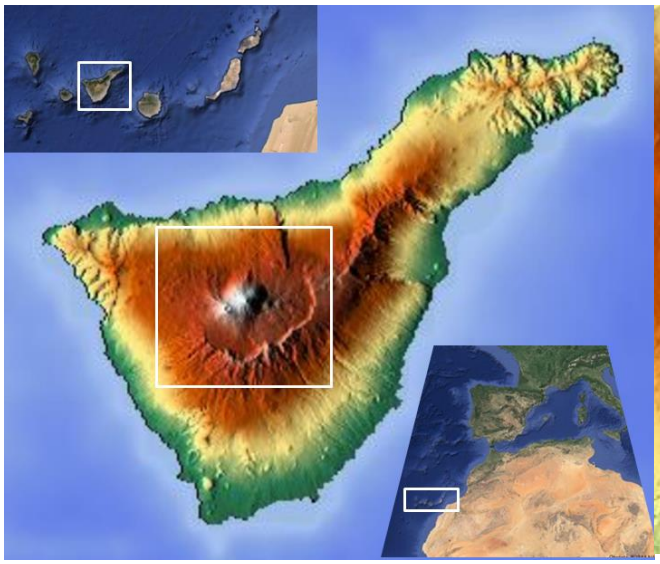

Figure 1a
Geographical location and topography of the Tenerife island, the largest and central island of the Canary islands (Spain) archipelago about 200 km westward of the coast of Morocco (Africa), with the central volcanic complex (CVC) dominated by the Teide summit (N 28.27°, W 16.6°, 3718 m a.s.l.). Rectangle delineates the area of the CVC portrayed in Fig. 1b.

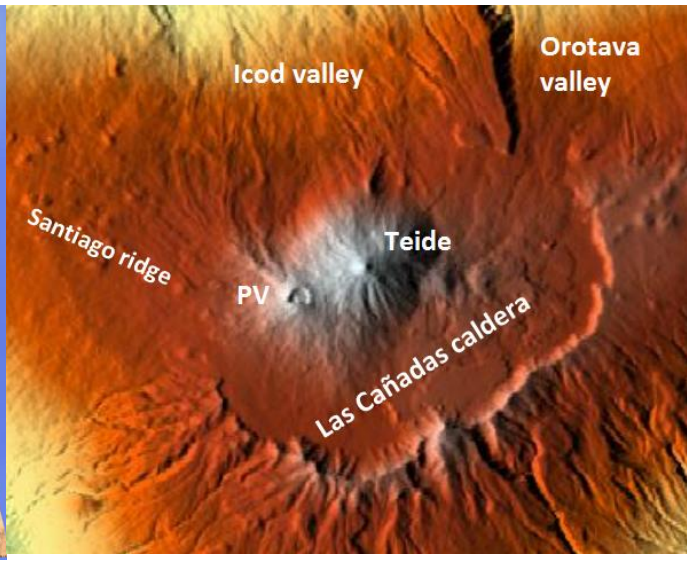

Figure 1b
The CVC with twin stratovolcanoes Teide and Pico Viejo (PV) located inside the Las Cañadas caldera (LCC) that is roughly 16 km wide. The Santiago ridge correspons with the NW (Santiago) rift zone (SRZ) characterized by vents respective to fissure-type eruptions.

Prutkin Ilya, Peter Vajda, Jo Gottsmann, 2014. The gravimetric picture of magmatic and hydrothermal sources driving hybrid unrest on Tenerife in 2004/5. *Journal of Volcanology and Geothermal Research*, 282: 9–18,
doi 10.1016/j.jvolgeores.2014.06.003 **preprint**
Final published ms (e-offprint): http://www.sciencedirect.com/science/article/pii/S0377027314001784

2. Observations and data reduction

A joint ground deformation/microgravity network was installed on the island in early May 2004, two weeks after the start of increased seismicity. The network consists of 14 benchmarks, which were positioned to provide coverage of a rather large area (> 500 km^2) of the CVC, including the Pico Viejo-Pico Teide complex (PV—PT), the Las Cañadas caldera (LCC) as well as the Santiago Rift (SR) (Fig. 1). The network was designed such that it can be fully occupied to a precision of better than 10 μGals of individual gravity readings between the reference and each benchmark and less than 4 cm in positioning errors within 6 working days despite the frequently rugged terrain. The first reoccupation of the network was performed in July 2004, followed by campaigns in April 2005 and July 2005. All measurements are reported with respect to a reference located south of the LCC (benchmark LAJA). Within the average precision of benchmark elevation measurements (± 3 cm), using two dual-frequency GPS receivers during each campaign, we did not observe widespread ground deformation. However, between May 2004 and July 2005, four benchmarks, two located in the eastern sector of the LCC (MAJU and RAJA), one marking the northern-most end of the network and also the lowest elevation (766 m; CLV1) and finally a benchmark located on an isolated rock spur on the western LCC rim (UCAN) did show ground uplift above measurement precision. To compute residual gravity changes, raw data were corrected for the theoretical free-air effect based on recorded changes in benchmark elevation, as well as Earth and Ocean tide effects and water table fluctuations.

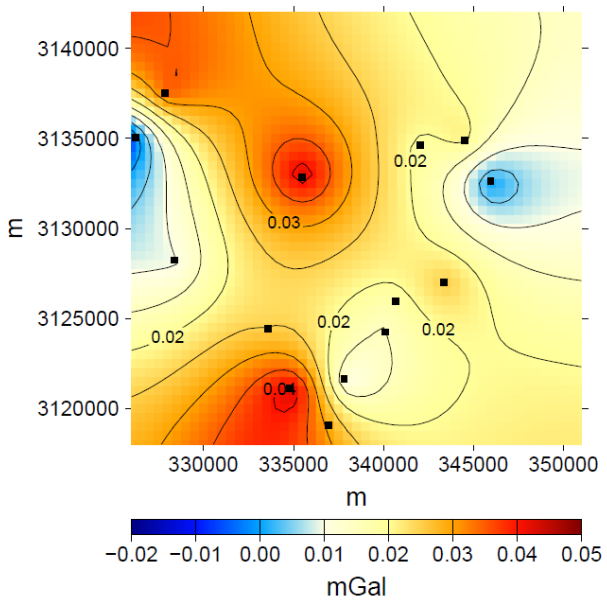

Figure 2
Gravity changes at the CVC (Fig. 1b) from May 2004 to July 2005 [mGal, 1 mGal = 10^{-5} m/s^2] corrected (reduced) for water table changes and local site effects, interpolated (extrapolated) onto a regular grid. Benchmarks are shown as little black squares. Coordinates are UTM easting and northing [m].

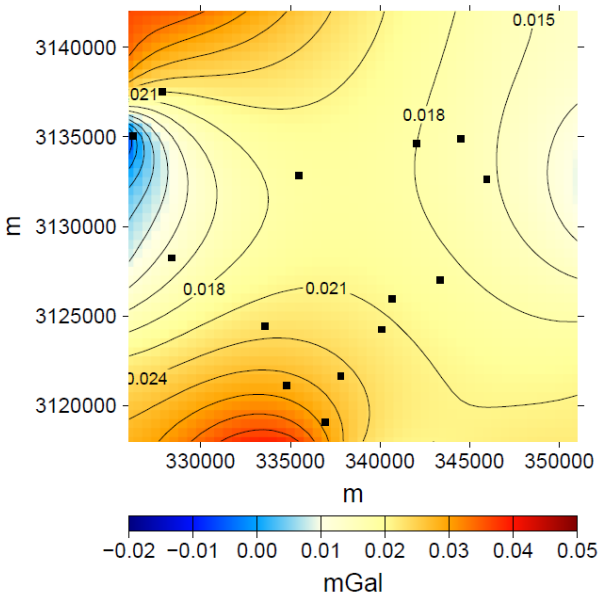

Figure 3
Trend [mGal]. Little black squares represent benchmarks. Horizontal coordinates are UTM easting and northing [m].

Data from two drill holes, located in the eastern half of the LCC provide information on water table fluctuations during the period of interest. A drop of about 5 cm/month between surveys 1 and 4 was recorded in one drill hole located close to benchmarks 3RDB and MAJU, which is similar to the average monthly drop in water level due to anthropogenic extraction over the past 3 years (Farrujia et al., 2004).

Prutkin Ilya, Peter Vajda, Jo Gottsmann, 2014. The gravimetric picture of magmatic and hydrothermal sources driving hybrid unrest on Tenerife in 2004/5. *Journal of Volcanology and Geothermal Research*, 282: 9–18,
doi 10.1016/j.jvolgeores.2014.06.003 **preprint**
Final published ms (e-offprint): http://www.sciencedirect.com/science/article/pii/S0377027314001784

Water levels decreased by 22 cm/month on average between February 2000 and January 2004 in a drill hole located close to benchmark MIRA. The gravity decrease of 25 μGal recorded between May 2004 and July 2005 at benchmark MIRA, located at the intersection of the Las Cañadas caldera and the Orotava valley, can be explained by a net water table decrease (δh) of 3 m, consistent with this earlier trend, assuming a permeable rock void space (φ) of 20 % and a water density (ρ) of 1000 kg/m^3 ($\Delta g_w = 2\pi G \rho \varphi \delta h$), cf. (Battaglia et al., 2003). Following the same rationale, raw gravity changes at 3RDB and MAJU are corrected by –8 μGal to account for the recorded water table fall in the nearby borehole. Hence, any gravity change observed within the central and eastern parts of the LCC (3RDB, MAJU, RAJA, MIRA) can be fully attributed to changes in (shallow) groundwater levels and we treat the net residual mass change as zero for this area.

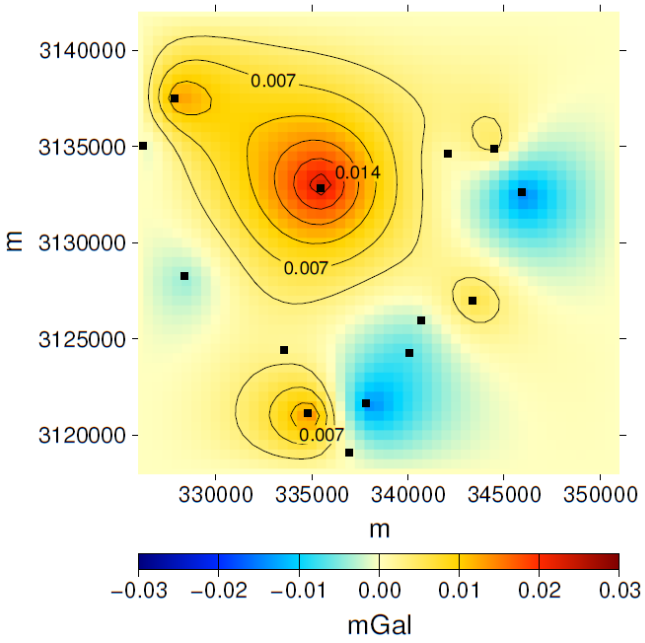

Figure 4
Residual gravity changes [mGal] after removal of the trend (Fig. 3). The two low amplitude gravity lows in the eastern and southern parts of the LCC are considered residues of site effects, thus remain unmodeled. Benchmarks are shown as little black squares

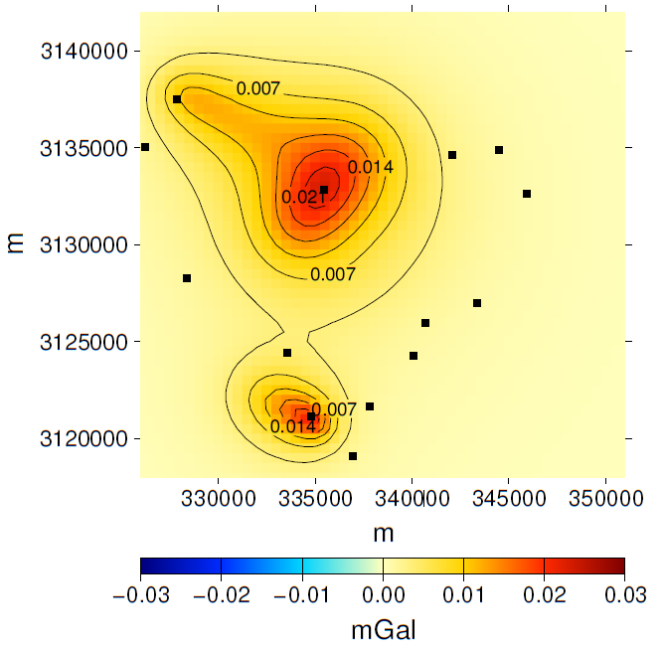

Figure 5
Gravitational effect [mGal] of the three line segments approximating the residual gravity changes (Fig. 4). The line segments represent sources of mass changes. Benchmarks are shown as little black squares.

Outside the LCC, comprehensive monitoring data on groundwater level is lacking and correction for groundwater level variations is difficult. Groundwater is collected and extracted along several hundred (sub)horizontal tunnels (gallerias) protruding into the upper slopes of the CVC (Marrero et al., 2005). Since 1925, a decrease of several hundred meters in the groundwater level has been noted for the area covered by the northern and western slopes of the CVC [http://www.aguastenerife.org/]. We therefore consider it very unlikely that the gravity increase noted in the north and west of the CVC is related to an increase in the groundwater table, and hence infer deeper processes to be the most probable cause of gravity change in this region. Additional details on the survey protocols and all measurement data are available from Gottsmann et al. (2006).

The reduced gravity changes (Appendix A), obtained after correction for elevation changes and water table changes, were interpolated/extrapolated over a regular grid with a spacing of 500 m (Fig. 2; 1 mGal = 10^{-5} m/s^2). We have used the "surface" code of the GMT software, which adopts gridding with

continuous curvature splines in tension (Smith and Wessel, 1990), providing the smoothest possible surface which interpolates given values. An equidistant data grid is needed to facilitate a triple harmonic continuation applied later during the data interpretation process. Next, a trend (Fig. 3) was removed from the gravity changes, resulting in the "residual gravity changes" (Fig. 4). The trend is a surface defined within the study area as a 2-D harmonic function constrained on the boundary of the study area by the extrapolated reduced gravity changes. Such trend is the smoothest possible function with prescribed values on the boundary, having no extrema (local highs or local lows) within the study area (Prutkin et al., 2011, section 2). The need to remove a trend is invoked by the subsequent application of signal decomposition by means of the triple harmonic continuation. The trend removal forces the residual gravity changes to become zero on (and beyond) the boundary of the study area. This property of the residual gravity changes is essential in our inversion process for two reasons: 1) it reduces the edge effects, i.e., the signal of sources from outside of the data (study) area, 2) it eliminates truncation errors in the triple harmonic continuation.

3. Inversion procedure and signal decomposition

In the inversion procedure the residual gravity changes are approximated by the gravitational effect (attraction) of 3D line segments. The gravitational effect (vertical derivative of the gravitational potential) of a line segment is given by a simple algebraic formula described by 7 parameters, twice the triplet of the end point coordinates plus a line density (Vajda et al., 2012, section 2.1). These parameters of the segments are determined by minimizing residuals in L_2 norm by means of non-linear minimization procedure, using the gradient method of Fletcher and Powell (1963). In the case of observed (residual) gravity changes, the set of the line segments represents the sources of the temporal mass/density changes, in terms of depth, length, orientation, and strength (i.e., the "line density") of each segment. The "line density" times the length of the segment amounts to the temporal mass change of the source. A positive mass change indicates the addition of subsurface mass.

As we will show in section 4.1, the initial inversion results are suspected to represent a composite picture of shallow- and deep- sources. To test this hypothesis, we decomposed the residual gravity changes shown in Fig 4 into a component generated by deep-seated sources, referred to as "deep field", and a counterpart generated by shallow-seated sources, referred to as "shallow field". The division level of 4 km b.s.l. (6 km below the "data surface") was chosen to roughly match the upper boundary of the two seismogenic zones of Cerdeña et al. (2011). The decomposition procedure is described in Appendix B. The two fields were then inverted separately yielding decomposed sources: shallow and deep line segments described in section 4.2.

4. Results and Interpretation

4.1 Three line segments and their interpretation

We achieved a fit (with rms of 3 μGal) to the residual gravity changes with a model of three line segments. The gravitational effect of the three segments, denoted as "line segments field" is shown in Fig. 5. The two low amplitude gravity lows in the eastern and southern parts of the LCC are considered residuals of site effects, and remain unmodelled. The positions, sizes, orientation, and mass changes of the three line segments are reported in Table 1 and displayed in Fig. 6. The estimated precision of the determined line segment end point coordinates is a few hundred meters.

The resultant line segments form a Z-shape in plan view (Fig. 6a). Two weaker line segments, with matching NW–SE strikes, border a central strong NE–SW striking line segment to the NW and SW. The central segment dips towards the NW from 1 km b.s.l. to 1.8 km b.s.l. Its center is located about 5 km to the north of the PV summit. The NW line segment follows the strike of the SRZ at a distance of about 5 km to the

north of the center line of SRZ at depths similar to the central segment, dipping towards SE. The shallow and weak segment in the SW is situated at depths between sea level and 1 km a.s.l., and runs parallel to the southwestern rim of the LCC.

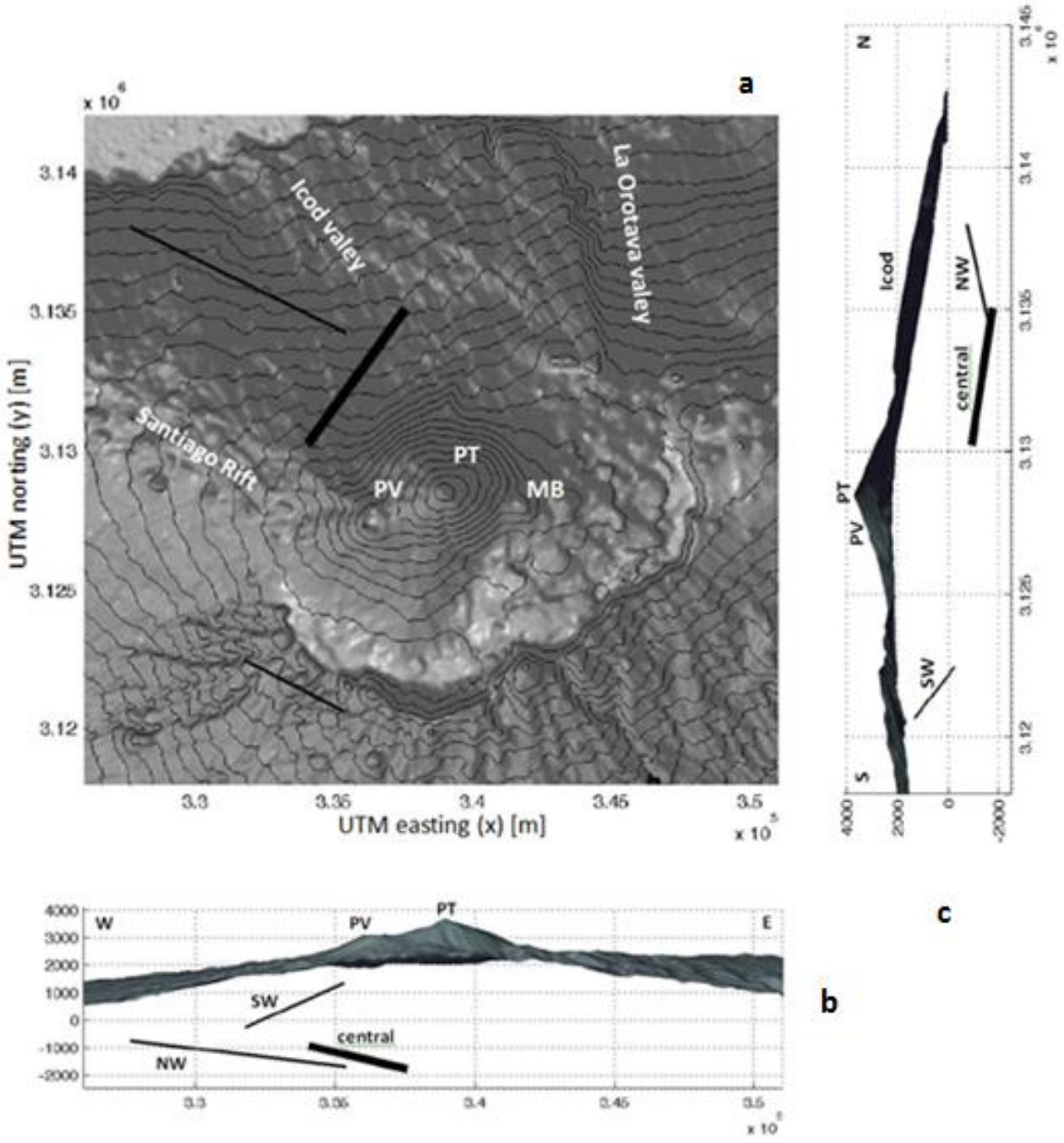

Figure 6
Positions, sizes, strengths, and orientation of the found three line segments within the CVC: (a) plan view, (b) W–E cross section, (c) S–N cross section (PV = Pico Viejo, PT = Pico Teide and MB = Montaña Blanca). The NW line segment dips towards the PV–PT complex, the central segment dips towards NE, and the SW line segment dips towards NW.

Prutkin Ilya, Peter Vajda, Jo Gottsmann, 2014. The gravimetric picture of magmatic and hydrothermal sources driving hybrid unrest on Tenerife in 2004/5. *Journal of Volcanology and Geothermal Research*, 282: 9–18,
doi 10.1016/j.jvolgeores.2014.06.003 **preprint**
Final published ms (e-offprint): http://www.sciencedirect.com/science/article/pii/S0377027314001784

Table 1. UTM coordinates X (easting) and Y (northing), and height (Z) with respect to sea level (positive means a.s.l., while negative means b.s.l.), all in [m], of the end points of the line segments, and their mass changes (δM in 10^{10} kg; positive values indicate subsurface mass addition.

line segment	X1	Y1	Z1	X2	Y2	Z2	δM
NW	335,410	3,134,200	- 1,720	327,660	3,137,990	- 770	+ 2.212
central	334,060	3,130,210	- 960	337,560	3,135,040	- 1,800	+ 5.509
SW	335,320	3,120,630	+ 1,310	331,770	3,122,450	- 300	+ 1.290

The central and NW line segments, as a couple, coincide horizontally with the NW seismogenic zone of Cerdeña et al. (2011), with depths focused along a line from 4 to 10 km b.s.l. and a mean depth of 7 km b.s.l., which roughly corresponds to the bottom of the basaltic shield of Tenerife. The NW seismogenic zone has a steeply dipping linear trend with a NE-SW strike. Horizontal location, as well as orientation, of the SW line segment coincides with the SW rim of the LCC. It lies close to the western caldera boundary fault, which is regarded as a pathway for fluids to shallower depth (Gottsmann et al., 2006). The horizontal location of the SW line segment coincides, at the same time, with the horizontal location of the SW seismogenic zone of Cerdeña et al. (2011) centered at the depth of about 4 km b.s.l. While we interpret the central and NW line segments as magmatic sources, the SW line segment may be associated with the movement of hydrothermal fluids.

We suspect, however, that two of the three line segments modeled above (the central and NW line segments) are a result of the superposition of shallow hydrothermal sources and deeper magmatic sources that could have triggered the rise of hydrothermal fluids. To test this hypothesis, we decomposed the gravimetric signal into shallow and deep fields, as described in section 3, to test for possible deeper (magmatic) sources.

4.2 Decomposition into shallow and deep line segments and their interpretation

The shallow and deep fields resulting from the decomposition are presented in Figures 7 and 8, respectively. Both fields are inverted. The inversion parameters for the obtained line segments respective to both fields are listed in Table 2. The estimated precision of the determined line segment end point coordinates is a few hundred meters. The line segments are presented in Fig. 9.

The deep field is approximated by two deep line segments (Dp1 and Dp2) with a RMS of 0.7 μGal. These two short deep segments lie at depths between 5.4 and 5.9 km b.s.l. The deep solution was constrained so that the deep line segments are connected at one of their endpoints. Such a constraint was chosen to reduce the number of inversion parameters. Alternatively we refer to the connected deep segments as a "bent deep segment" (Dp), cf. Fig. 9.

The two connected deep segments may be regarded as one single source, with a slightly arcuate geometry. The shallow field is approximated by three shallow line segments (ShNW1, ShNW2 and ShSW) with a RMS of 2.3 μGal. The three shallow-seated segments are located between 400 m and 1.4 km a.s.l.

Among the shallow segments, the ShSW segment is practically matching the SW line segment of the preceding solution of sec. 4.1 (cf. Fig. 6), and the two shallow-seated NW line segments (ShNW1/2) strike nearly parallel to the Santiago rift. The one closer to the PV-PT complex (ShNW1) is stronger, while its NW end is situated nearly straight above the deep line segment (Dp). Segment ShNW2 is weak and is modeled to lie partially above the surrounding terrain. This is an artefact caused by the choice of our reference level of 2 km a.s.l. for all residual gravity changes employed in the inversion. We therefore consider source ShNW2 to have a near-surface location.

Our interpretation of the deep bent segment (Dp) is that it represents a magma injection at a depth of about 5.5 to 6 km b.s.l. Reasons for such interpretation are discussed in the below section. By contrast,

the three shallow segments are inferred to represent propagation of hydrothermal fluids/gases as a result of the deeper magma migration.

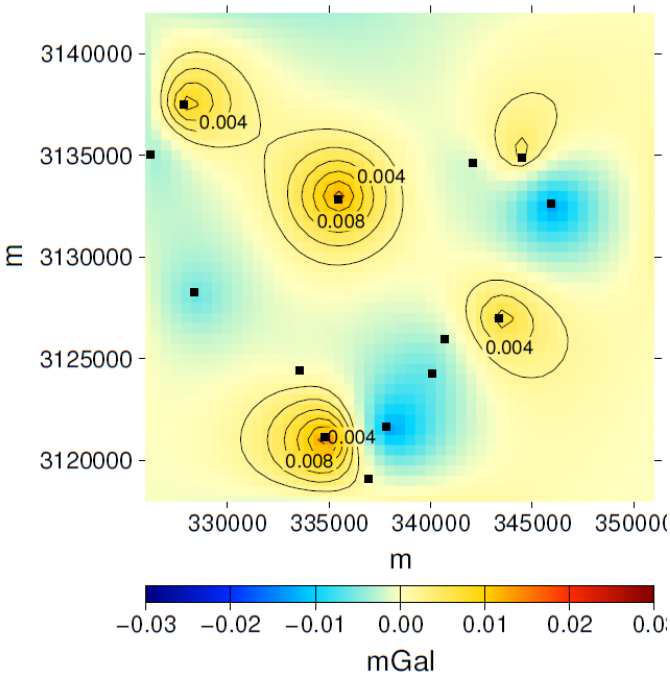

Figure 7
Shallow field [mGal] resulting from the decomposition of the residual gravity changes (Fig. 4). Benchmarks are shown as little black squares.

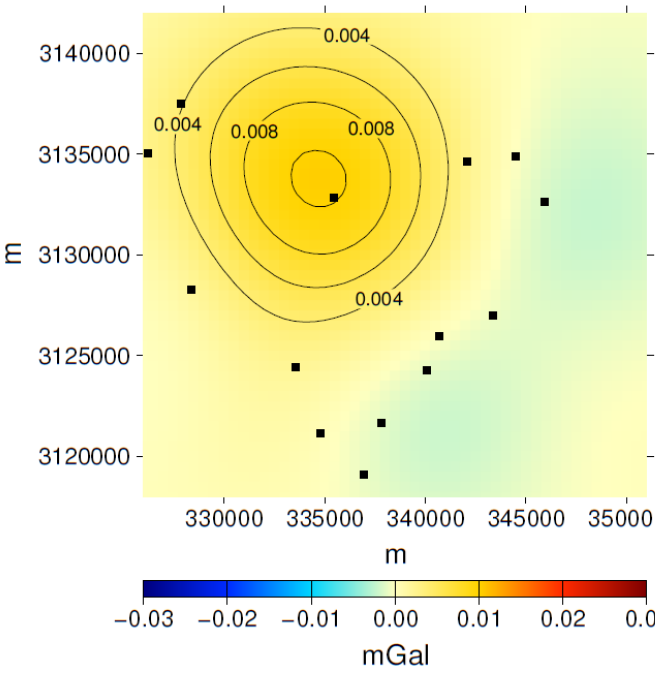

Figure 8
Deep field [mGal] resulting from the decomposition of the residual gravity changes (Fig. 4). Benchmarks are shown as little black squares

Table 2. UTM coordinates X (easting) and Y (northing), and height (Z) with respect to sea level [m] of the end points of the shallow (Sh) and deep (Dp) sources represented by line segments, and their mass changes (δM), positive meaning mass addition [10^{10} kg].

line segment	X1	Y1	Z1	X2	Y2	Z2	δM
ShNW1	336,560	3,132,050	590	334,210	3,134,040	420	+ 0.83
ShNW2	327,500	3,137,930	1,280	330,330	3,137,260	600	+ 0.31
ShSW	335,460	3,120,730	1,380	332,100	3,121,210	380	+ 0.53
Dp1	334,890	3,133,910	- 5,440	334,630	3,134,200	- 5,680	+ 7.25
Dp2	334,310	3,134,590	- 5,840	334,630	3,134,200	- 5,680	+ 8.24

Upon the decomposition we see no sources (no significant mass input) within the area assumed to comprise the shallow phonolitic magmatic system of the PV–PT complex. This finding is discussed below in the context of other geoscientific findings reported for the 2004/5 unrest period at the CVC.

Prutkin Ilya, Peter Vajda, Jo Gottsmann, 2014. The gravimetric picture of magmatic and hydrothermal sources driving hybrid unrest on Tenerife in 2004/5. *Journal of Volcanology and Geothermal Research*, 282: 9–18,
doi 10.1016/j.jvolgeores.2014.06.003 **preprint**
Final published ms (e-offprint): http://www.sciencedirect.com/science/article/pii/S0377027314001784

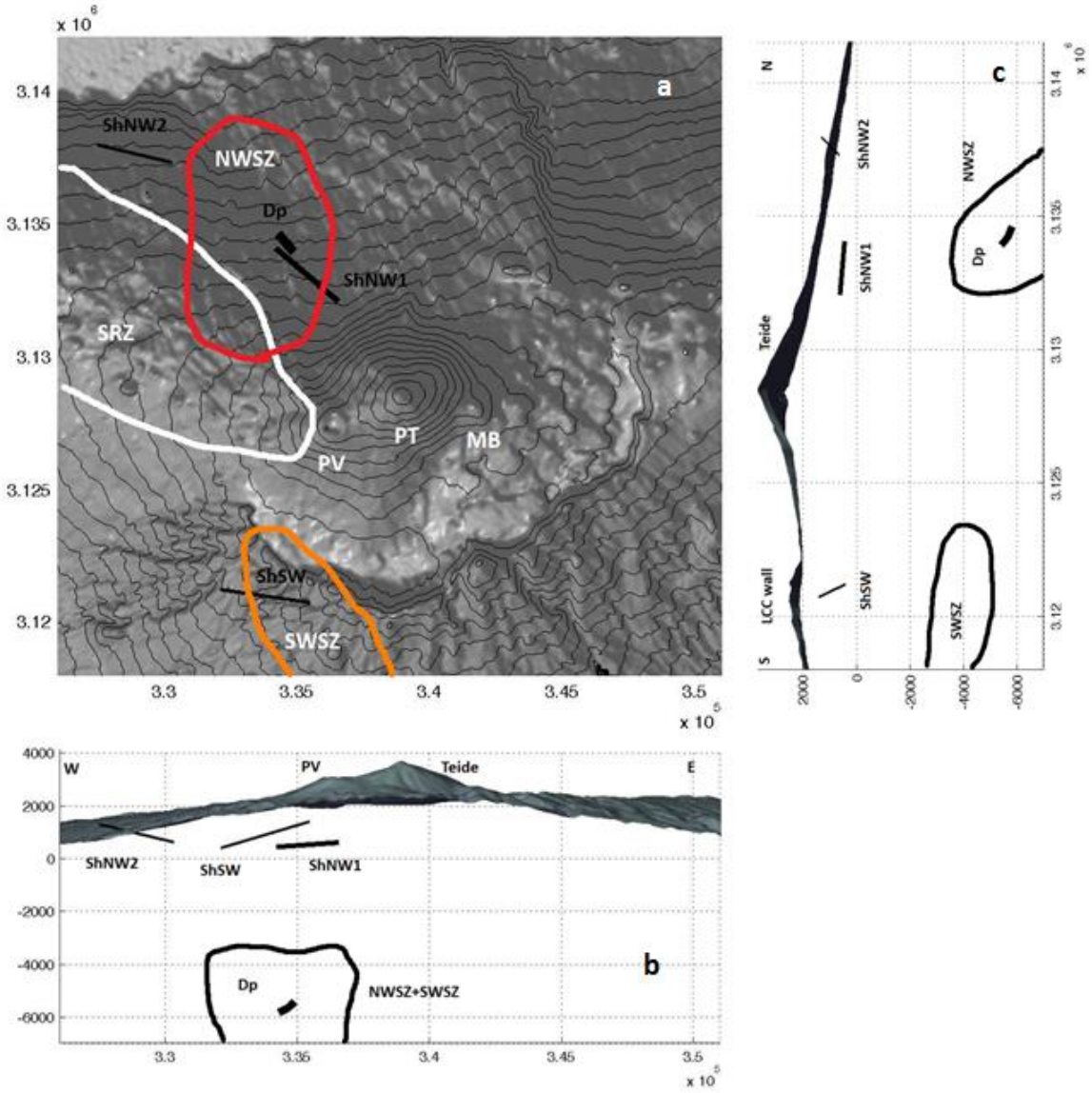

Figure 9

Positions, sizes, strengths, and orientation of the shallow (ShNW1, ShNW2, and ShSW) and deep (Dp) line segments respective to the decomposed residual gravity changes: (a) plan view, (b) W–E cross section, (c) S–N cross section. The Santiago (NW) rift zone (SRZ) marked in plan view delineates the zone of past fissure eruptions and mafic vents including the historic eruptions: Montañas Negras in 1706, Chahorra in 1798 and El Chinyero in 1909 (cf. Fig. 2 of Cerdeña et al. (2011)). Between May 2004 and July 2005 the SRZ was characterized by anomalously high CO_2 degassing. The NW and SW seismogenic zones (cf. Fig. 6 of Cerdeña et al. (2011)) are schematically delineated ("NWSZ" and "SWSZ", respectively) within the CVC comprised of Teide (PT), Pico Viejo (PV), Montaña Blanca (MB) and the caldera (LCC).

5. Discussion

We have performed the analysis of the precision (uncertainty) of the inversion results parameters (endpoints of line segments as well as their masses) by linearizing the nonlinear inverse problem in terms of Taylor series expansion at an origin located approximately at the center of the shallow line segments cluster, to estimate the precision of the shallow line segments, and at an origin located approximately at the center of

the deep segments cluster, to estimate the precision of the deep line segments. The resulting precision (uncertainty) estimates are tabulated in a supplementary material. Uncertainty for endpoints of shallow segments ranges in horizontal position from 590 meters to 1 830 m, and in vertical position from 430 m to 950 m, while for deep segments it ranges in horizontal position from 130 m to 160 m and in vertical position from 150 m to 400 m. The uncertainty estimation using the Taylor series expansion might be too optimistic for the deep segments. We prefer to speak of the estimated model uncertainty amounting to several hundred meters.

The inversion of the decomposed gravimetric signals recorded during the 2004–2005 unrest of the CVC on Tenerife leads to the interpretation of magma intruding to a depth of at least 6 km b.s.l. at the center of the NW seismogenic zone (Cerdeña et al., 2011), roughly 5 km to the NNW of the Pico Viejo. The release of magmatic fluids from the intrusion through a network of permeable pathways or zones of least resistance into shallow-seated hydrothermal systems can explain the dynamics in the shallow secondary sources deduced by the inversion. Alternatively, subsurface stress changes associated with the intrusion triggered activity in shallow seated hydrothermal aquifers in the NW and the SW, without direct input of juvenile fluids from the intrusion. That said we do need a net mass input in those sources to explain the gravity signal. One such shallow source appears situated directly above the intrusion, while two other zones are imaged to the NW and the SW (Fig. 9). Next we compare our interpretation to other published works regarding the 2004/5 unrest.

Gottsmann et al. (2006) interpreted the spatio-temporal changes in gravity as a migration of hydrothermal fluids, possibly triggered by a deeper magma recharge NW of the CVC. They suggest a model of an anomalous mass increase with N-S strike to the west of PV at a depth of roughly sea level. Our interpretation correlates with this scenario in that our results indicate a magma injection at depth of roughly 6 km b.s.l. in the NW zone, and a vertical rise of hydrothermal fluids straight above the injection followed by lateral migration towards the NW along the SRZ, and towards the SW along the SW rim of the LCC. Compared to the model results of Gottsmann et al. (2006), we constrain the areas into which fluids were injected to a shallower depth, and closer to the surface of the caldera and SRZ.

Almendros et al. (2007) provide a similar model to explain the unrest based on analyzing three weeks of continuous data at three seismic antennas deployed at the LCC. In their interpretation a magmatic reactivation started in April 2004 on the NW flank of PT at depths below 14 km (referenced to the edifice surface). The subsequent magma degassing initiated the rise of volatiles, which later reached the aquifer of the caldera.

Cerdeña et al. (2011) propose a different model scenario for the unrest. They report alternating activity between the SW and NW seismogenic zones, which supposedly points to an internal link between them. They believe this fact refutes the theory of a gradual migration from N to S reported by Almendros et al. (2007) and Martí et al. (2009). Although more than 95% of the seismic energy was released by the NW seismogenic zone, Cerdeña et al. (2011) propose a four stage tree-like magma intrusion model to explain the 2004 seismo-volcanic unrest. In their model, which covers the time span 2001–2004, magma ascended from greater depth at a central location below PT and was injected sideways into the NW and SW seismogenic zones, being controlled by the NW (along the Santiago) and NE (along the Dorsal) rifts. Diking is interpreted to have produced the VT swarms observed in their seismic records. Our model interpretation partly correlates with their intrusive model inasmuch as the location of the deep anomalous gravimetric source (Dp) matches the center of their NW seismogenic zone. In addition, the shallow-seated SW hydrothermal source imaged by both our models matches the horizontal position of their SW seismogenic zone. However, we cannot find/see any gravimetric signature of the central vertical magma conduit proposed in their tree-like magma intrusion model reaching the shallow phonolitic magma chambers just below the PV–PT complex.

Based on new phase equilibrium experiments of the most recent magmas erupted from Pico Teide and its satellite vents, Andújar et al. (2010, 2013) estimate the depth of the magma chambers at 1–2 km beneath the surface for the satellite eruptions and 5 km beneath the surface (1–2 km b.s.l.) for central

eruptions. Although the vertical position of our strong central line segment shown in Fig. 6 matches the petrologically determined depths of the phonolitic magma reservoirs beneath the PV–PT complex, it is offset by about 5 km northward of PT. The inversion of the decomposed gravity field demonstrates that this source may in fact be a composite apparent image of the near-vertical superposition of a deep-seated source and a shallow-seated source. Upon decomposition we found the magmatic source responsible for the observed gravity to be seated at a depth of about 6 km b.s.l, well deeper than the proposed depth of the phonolitic magma chambers of the PV–PT complex. This has important implications for the interpretation of unrest processes at the CVC as rejuvenation of the phonolitic magma reservoir by mafic inputs has been proposed as past eruption trigger (e.g., Araña et al. 1994; Martí et al., 2008; Andújar and Scaillet, 2012). Based on the results presented herein there is no indication from the gravimetric data for a significant mass addition to the phonolitic reservoirs beneath the CVC during the 2004/5 unrest.

When we accept that the migration of hydrothermal fluids played a significant role during the unrest, for which the geophysical evidence is convincing, i.e., that the unrest was hybrid rather than purely magmatic or purely hydrothermal, then we have to consider our inversion results of section 4.2 more realistic than those of section 4.1. The shallow-seated line segments found in the NW portion of the survey area (cf. Fig. 9) match the average strike of the SRZ along which volcanic eruptions over the past few centuries were dominantly fed by basic and intermediate magmas in the form of fissure eruptions (Ablay and Martí, 2000). This might hint towards the presence of a zone of increased permeability, which facilitates the propagation of hydrothermal fluids released from depth. The recent inversion of static gravity data from the CVC by Gottsmann et al. (2008) also provides compelling evidence for a structural control of shallow fluid flow in the CVC. Their model identifies pronounced low-density anomalies in the locations of the weak NW and SW line segments, which could indicate preferred pathways for fluid migration.

With respect to degassing and fumarolic activity associated with the magmatic-hydrothermal system of the CVC during the seismic–volcanic crisis Melián et al. (2012) note that it had significant effects on the magmatic–hydrothermal system of Teide Volcano, as deduced from the temporal evolution of degassing activity at the summit crater. Noticeably, a higher contribution of magmatic gases accompanied by enhanced total diffuse CO_2 emissions was observed. Galindo (2005) and Marti et al. (2009) report an increase in CO_2 flux along the SRZ during the crisis, while García et al. (2006) report a fumarolic plume at the summit of Teide visible to the naked eye for a few hours on 20 October 2004. Pérez et al. (2013) state that other geochemical precursors of this seismic–volcanic unrest were also observed in the local aquifer, such as an increase in radon in the proximity of the south rift-zone of the island around the middle of 2003, and an increase in the SO_4/Cl ratio in the groundwater of the Hoya de la Leña gallery in April 2004. They express that these geochemical changes suggest a magmatic fluid injection into the Teide hydrothermal system in 2004 caused by deep magma movement beneath the Teide volcanic system. They also claim that the chemical composition of fumarolic gases reported by Melián et al. (2012) and the low SO_2 emission data measured by Weber et al. (2006) do not support the hypothesis of the (re)-activation of the phonolitic Teide–Pico Viejo magmatic system. Our analyses indicating an absence of mass input into the central phonolitic plumbing system of the PT–PV complex are in good agreement with this inference.

De Barros et al. (2012) identify and analyze seismic anomalies possibly associated with the magmatic system of the CVC using scattered seismic wavefields based on a double beam-forming analysis hinging on a 3D tomographic model for Tenerife (García-Yeguas et al., 2012). This technique is deemed reliable for locating scattering structures at depth, even when the velocity model is imperfect. Two main anomalies were identified: a deeper anomaly (approximately 5–10 km b.s.l.) in the northern part (3115–3140 km UTM) of the S–N cross section running through the Teide summit, and a shallower anomaly (1–4 km b.s.l.) in the W–E cross section right beneath the Teide summit. They interpret the shallow anomaly as possibly pertinent to the phonolitic storage area feeding the Teide-Pico Viejo complex, while the deeper anomaly as possibly related to the basaltic feeder system. They mention two possibilities in their interpretation: these anomalous seismic regions represent either fractures filled by volatiles associated with the gas-filled upper part of the magma storage system, or a complex set of dykes and sills filled with magma. Their deeper northern

anomalous structure correlates well with the NW seismogenic zone of Cerdeña et al. (2011). Our deep bent line segment (Dp of Fig. 9) correlates with both of them.

6. Conclusions

In potential field inverse problems we often deal with composite signals while the decomposition into multiple sources inherently remains an ambiguous task. Here, we show the decomposition of the gravity changes observed during the 2004–2005 unrest at the CVC of Tenerife in the context of all presently available data and geoscientific cognition, in order to gain insights into the processes that generated the recorded signals. Our gravimetric model of the 2004 unrest at the CVC on Tenerife indicates a magma intrusion at the depth of about 6 km b.s.l. along the strike and dip of the NW seismogenic zone. The intrusion initiated the release of volatiles and/or stress changes that drove hydrothermal fluids towards the shallow subsurface along zones of structural weakness in the western-most part of the Las Cañadas caldera and along the Santiago rift zone. The nature of the unrest is hence best termed as hybrid.

The three most recent historic eruptive episodes on Tenerife were lower Santiago and Dorsal rifts eruptions (1704–1705, 1706, 1909) and the eruption of Pico Viejo in 1798. The last two eruptions indicate continued input of fresh magmas into the shallow rift system from a deep storage zone (Ablay and Martí, 2000). The time span in-between these three eruptions is roughly a century (93 and 111 years, respectively). Conspicuously enough, the 2004 unrest follows a similar repeatability pattern (95 years after Chinyero). We may consider the 2004 hybrid unrest on Tenerife a failed eruption.

Acknowledgements
JG acknowledges support from a Royal Society University Research Fellowship (grant No. UF090006) and from the EC FP7 project “VUELCO” (grant #: 282759). PV was supported by the Slovak Research and Development Agency under the contract No. APVV-0724-11 and by Vega grant agency under projects No. 2/0067/12 and 1/0095/12.

Appendix A – Data

Reduced gravity changes observed at the 14 benchmarks, corrected for water table changes and local site effects (Gottsmann et al., 2006), are listed below.

Benchmark	x (m)	y (m)	z (m)	δg (mGal)
3RDB	340,088.27	3,124,255.73	2,223.83	0.015
C774	326,223.80	3,135,041.90	1,129.87	- 0.005
CHIO	328,395.66	3,128,241.55	1,641.38	0.010
CLV1	327,850.19	3,137,504.73	766.69	0.034
CRUC	335,456.99	3,132,853.45	1,577.25	0.042
FUEN	344,517.31	3,134,882.63	1,723.90	0.021
KLM3	333,563.77	3,124,426.17	2,132.04	0.025
LAJA	336,950.69	3,119,087.14	2,115.85	—
LLAN	337,814.75	3,121,655.61	2,068.12	0.011
MAJU	340,689.82	3,125,959.81	2,362.13	0.018
MIRA	345,959.30	3,132,627.14	2,037.48	0.001
RAJA	343,375.08	3,126,992.68	2,363.57	0.025
TORR	342,058.62	3,134,638.45	1,755.26	0.019
UCAN	334,784.50	3,121,120.25	2,155.18	0.042

Prutkin Ilya, Peter Vajda, Jo Gottsmann, 2014. The gravimetric picture of magmatic and hydrothermal sources driving hybrid unrest on Tenerife in 2004/5. *Journal of Volcanology and Geothermal Research*, 282: 9–18,
doi 10.1016/j.jvolgeores.2014.06.003 **preprint**
Final published ms (e-offprint): http://www.sciencedirect.com/science/article/pii/S0377027314001784

Appendix B – Decomposition into shallow and deep fields

The field (residual gravity changes δg^r) is decomposed into shallow and deep parts (fields) as follows. The deep field is defined as a field harmonic down to depth *d* below the surface at which the data δg^r are given (a level of average altitude of the benchmarks). As the deep field is harmonic down to depth *d*, it is generated exclusively by sources below the depth *d*. The deep field is computed by subsequent upward–downward–upward harmonic continuations.

First, we continue the data $\delta g^r(x,y,0)$ upward to a height (above the data surface) $h = d$ to attenuate the signal of sources in the near-surface layer. The upward continuation is performed by means of the Poisson integral (in planar approximation)

$$\frac{1}{2\pi}\iint_S \frac{d}{[(x-x')^2+(y-y')^2+d^2]^{3/2}}\delta g^r(x,y,0)dxdy = \delta g^r(x',y',d) \tag{1}$$

The above formula represents the solution of a direct problem, the Dirichlet problem. It is solved by numerical evaluation of the Poisson surface integral. Note that the data $\delta g^r(x,y,0)$ over which the surface integration is performed are zero on and beyond the boundary of our study area *S* due to the removal of the trend, which eliminates truncation errors that would otherwise be introduced by truncating the integration domain from the entire earth surface to the area of *S*. Second, we continue the obtained data $\delta g^r(x',y',d)$ downward over a distance 2*d*, i.e., to the depth *d* below the data surface

$$\frac{1}{2\pi}\iint_S \frac{2d}{[(x-x')^2+(y-y')^2+(2d)^2]^{3/2}}\delta g^r(x,y,-d)dxdy = \delta g^r(x',y',d) \tag{2}$$

This step represents an inverse problem. Now we have to, and we do, treat the formula as an integral equation: the right hand side $\delta g^r(x',y',d)$ is given, while the unknown function $\delta g^r(x,y,-d)$ on the left hand side is sought. Let us write the discretized form of the above integral equation as $\boldsymbol{A\delta g^r}(-d) = \boldsymbol{\delta g^r}(d)$, where $\boldsymbol{A}$ is the design matrix, $\boldsymbol{\delta g^r}(-d)$ is the vector of unknowns, and $\boldsymbol{\delta g^r}(d)$ is the vector of given values. This is a linear ill-posed inverse problem, which requires regularization. Since the design matrix $\boldsymbol{A}$ is self-adjoint and positive, we apply the Lavrent'ev's approach (Lavrent'ev et al., 1986) to regularize the problem: $(\boldsymbol{A}+\alpha\boldsymbol{I})\boldsymbol{\delta g^r}(-d) = \boldsymbol{\delta g^r}(d)$, where $\boldsymbol{I}$ is identity matrix, and α is regularization parameter.

Third, we upward continue the data, over a distance *d*, back to the data surface, which is numerically the same procedure as the first upward continuation already described. By this triple harmonic continuation procedure we derive the deep field, which is a part of the residual gravity changes that is harmonic down to the depth *d* (below the data surface). Therefore, the deep field can be treated as the gravitational effect of sources residing below the depth *d*.

The shallow field is obtained by subtracting the deep field from the original field (from the residual gravity changes). Now the shallow field can be considered as the gravitational effect of sources between the surface and the level of depth *d*. This decomposition procedure using the triple harmonic continuation has been successfully applied in several gravimetric studies ranging from local/regional to global (Prutkin, 2008; Prutkin and Casten, 2009; Prutkin and Saleh, 2009; Prutkin et al., 2011).

Prutkin Ilya, Peter Vajda, Jo Gottsmann, 2014. The gravimetric picture of magmatic and hydrothermal sources driving hybrid unrest on Tenerife in 2004/5. *Journal of Volcanology and Geothermal Research*, 282: 9–18,
doi 10.1016/j.jvolgeores.2014.06.003 **preprint**
Final published ms (e-offprint): http://www.sciencedirect.com/science/article/pii/S0377027314001784

References

Araña, V., Martí, J., Aparicio, A., García-Cacho, L., García-García, R., 1994. Magma mixing in alkaline magmas: An example from Tenerife, Canary Islands. Lithos 32(1–2), 1–19.

Ablay, G.J., Martí, J., 2000. Stratigraphy, structure, and volcanic evolution of the Pico Teide–Pico Viejo formation, Tenerife, Canary Islands. J. Volcanol. Geotherm. Res., 103(1–4), 175–208, doi: 10.1016/S0377-0273(00)00224-9.

Almendros, J., Ibáñez, J.M., Carmona, E., Zandomeneghi, D., 2007. Array analyses of volcanic earthquakes and tremor recorded at Las Cañadas caldera (Tenerife Island, Spain) during the 2004 seismic activation of Teide volcano. J. Volcanol. Geotherm. Res., 160(3–4), 285–299, doi: 10.1016/j.jvolgeores.2006.10.002.

Andújar, J., Scaillet, B., 2012. Experimental Constraints on Parameters Controlling the Difference in the Eruptive Dynamics of Phonolitic Magmas: the Case of Tenerife (Canary Islands). Journal of Petrology 53(9), 1777–1806.

Andújar, J., Costa, F., Martí, J., 2010. Magma storage conditions of the last eruption of Teide volcano (Canary Islands, Spain). Bulletin of Volcanology 72, 381–395, doi: 10.1007/s00445-009-0325-3.

Andújar, J., Costa, F., Scaillet, B., 2013. Storage conditions and eruptive dynamics of central versus flank eruptions in volcanic islands: The case of Tenerife (Canary Islands, Spain). J. Volcanol. Geotherm. Res. 260, 62–79, doi 10.1016/j.jvolgeores.2013.05.004.

Battaglia, M., Segall, P., Roberts, C., 2003. The mechanics of unrest at Long Valley caldera, California. 2. Constraining the nature of the source using geodetic and micro-gravity data. J. Volcanol. Geotherm. Res, 127(3-4), 219–245, doi 10.1016/S0377-0273(03)00171-9.

Cerdeña Domínguez, I., del Fresno, C., Rivera, L., 2011. New insight on the increasing seismicity during Tenerife's 2004 volcanic reactivation. J. Volcanol. Geotherm. Res. 206, 15–29, doi: 10.1016/j.jvolgeores.2011.06.005.

De Barros, L., Martini, F., Bean, C.J., García-Yeguas, A., Ibáñez, J., 2012. Imaging magma storage below Teide volcano (Tenerife) using scattered seismic wavefields. Geophysical Journal International, 191(2), 695–706, doi 10.1111/j.1365-246X.2012.05637.x .

Farrujia, I., Velasco, J.L., Fernandez, J., Martin, M.C., 2004. Evolución del nivel freático en la mitad oriental del acuífero de Las Cañadas del Teide. Cuantificación de parámetros hidrogeológicos, in VIII Simposio de Hidrogeología de la Asociación Española de Hidrogeólogos, Zaragoza

Fletcher, R., Powell, M.J.D., 1963. A rapidly convergent descent method for minimization. The Computer Journal 6(2), 163–168, doi 10.1093/comjnl/6.2.163.

Galindo, I., 2005. Estructura volcano-tectónica y emisión difusa de gases de Tenerife (Islas Canarias). PhD Thesis, University of Barcelona, 350 pp.

García, A., Vila, J., Ortiz, R., Macia, R., Sleeman, R., Marrero, J.M., Sánchez, N., Tárraga, M., Correig, A.M., 2006. Monitoring the reawakening of Canary Islands' Teide Volcano, Eos Trans. AGU, 87(6), 61.

García-Yeguas, A., Koulakov, I., Ibáñez, J., Rietbrock, A., 2012. High resolution 3D P wave velocity structure beneath Tenerife Island (Canary Islands, Spain) based on tomographic inversion of active-source data. Journal of Geophysical Research, 117, B9, doi 10.1029/2011JB008970

Gottsmann, J., Wooller, L., Martí, J., Fernández, J., Camacho, A.G., Gonzalez, P.J., Garcia, A., Rymer, H., 2006. New evidence for the reawakening of Teide volcano. Geophys. Res. Lett., 33, L20311, doi:10.1029/2006GL027523

Gottsmann, J., Camacho, A.G., Martí, J., Wooller, L., Fernández, J., García, A., Rymer, H., 2008. Shallow structure beneath the Central Volcanic Complex of Tenerife from new gravity data: Implications for its evolution and recent reactivation. Physics of the Earth and Planetary Interiors 168(3–4), 212–230, doi 10.1016/j.pepi.2008.06.020.

Lavrent'ev, M.M., Romanov, V.G., Shishatskii, S.P., 1986. Ill-Posed Problems of Mathematical Physics and Analysis. Translations of Math. Monographs v. 64. Amer. Math. Soc, Providence.

Marrero, R., Salazar, P., Hernández, P.A., Pérez, N.M., López, D., 2005. Hydrogeochemical monitoring for volcanic surveillance at Tenerife, Canary Islands, Geophys. Res. Abstr., 7, Abstract 09928, sref-id: EGU05– A-09928

Martí, J., Geyer, A., Andújar, J., Teixido, F., Costa, F., 2008. Assessing the potential for future explosive activity from Teide-Pico Viejo stratovolcanoes (Tenerife, Canary Islands). J. Volcanol. Geotherm. Res. 178(3), 529–542, doi 10.1016/j.jvolgeores.2008.07.011.

Martí, J., Ortiz, R., Gottsmann, J., García, A., De La Cruz-Reyna, S., 2009. Characterising unrest during the reawakening of the central volcanic complex on Tenerife, Canary Islands, 2004–2005, and implications for assessing hazards and risk mitigation. J. Volcanol. Geotherm. Res. 182, 23–33, doi 10.1016/j.jvolgeores.2009.01.028

Melián, G., Tassi, F., Pérez, N., Hernández, P., Sortino, F., Vaselli, O., Padrón, E., Nolasco, D., Barrancos, J., Padilla, G., Rodríguez, F., Dionis, S., Calvo, D., Notsu, K., Sumino, H., 2012. A magmatic source for fumaroles and diffuse degassing from the summit crater of Teide Volcano (Tenerife, Canary Islands): a geochemical evidence for the 2004-2005 seismic-volcanic crisis. Bulletin of Volcanology, 74(6), 1465–1483, doi: 10.1007/s00445-012-0613-1.

Pérez, N.M., Melián, G., Galindo, I., Padrón, E., Hernández, P.A., Nolasco, D., Salazar, P., Pérez, V., Coello, C., Marrero, M., et al., 2005. Premonitory geochemical and geophysical signatures of volcanic unrest at Tenerife, Canary Islands, Geophys. Res. Abstr., 7, Abstract 09993, sref-id: EGU05–A-09993

Pérez, N.M., Hernández, P.A., Padrón, E., Melián, G., Nolasco, D., Barrancos, J., Padilla, G., Calvo, D., Rodríguez, F., Dionis, S., Chiodini, G., 2013. An increasing trend of diffuse CO_2 emission from Teide volcano (Tenerife, Canary Islands): geochemical evidence of magma degassing episodes. Journal of the Geological Society, London, 170(4), 585–592, doi 10.1144/jgs2012-125.

Prutkin, I., 2008. Gravitational and magnetic models of the core–mantle boundary and their correlation. Journal of Geodynamics 45(2–3), 146–153, doi 10.1016/j.jog.2007.09.001.

Prutkin, I., Casten, U., 2009. Efficient gravity data inversion for 3D topography of a contact surface with application to the Hellenic subduction zone. Computers & Geosciences 35(2), 225–233, doi 10.1016/j.cageo.2008.02.036.

Prutkin, I., Saleh, A., 2009. Gravity and magnetic data inversion for 3D topography of the Moho discontinuity in the northern Red Sea area, Egypt. Journal of Geodynamics 47(5), 237–245, doi 10.1016/j.jog.2008.12.001.

Prutkin I., Vajda P., Tenzer R., Bielik, M., 2011. 3D inversion of gravity data by separation of sources and the method of local corrections: Kolarovo gravity high case study. Journal of Applied Geophysics 75(3), 472–478, doi: 10.1016/j.jappgeo.2011.08.012.

Smith, W.H.F., Wessel, P., 1990. Gridding with continous curvature splines in tension. Geophysics, 55, 293–305.

Tárraga, M., Carniel, R., Ortiz, R., Marrero, J.M., García, A., 2006. On the predictability of volcano-tectonic events by low frequency seismic noise analysis at Teide-Pico Viejo volcanic complex, Canary Islands, Nat. Hazards Earth Syst. Sci., 6(3), 365–376.

Vajda, P., Prutkin, I., Tenzer, R., Jentzsch, G., 2012. Inversion of temporal gravity changes by the method of local corrections: A case study from Mayon volcano, Philippines. J. Volcanol. Geotherm. Res., 241–242, 13–20, doi 10.1016/j.jvolgeores.2012.06.020.

Weber, K., Fischer, C., Van Haren, G., Bothe, K., Pisirtsidis, S., Laue, M., González Ramos, Y., Barrancos Martínez, J., Hernández, P., Pérez, N., Pabel, K., Sosef, M., 2006. Ground-based remote sensing of gas emissions from Teide volcano (Tenerife, Canary Islands, Spain): First results. Proceedings SPIE 6362, Remote Sensing of Clouds and the Atmosphere, XI, 63621H, doi:10.1117/12.714411.